

A novel reformed histogram equalization based medical image contrast enhancement using krill herd optimization

Pankaj Kandhway^a, Ashish Kumar Bhandari^{a,*}, Anurag Singh^b

^a Department of Electronics and Communication Engineering, National Institute of Technology Patna, 800005, India

^b Department of Electronics and Communication Engineering, International Institute of Information Technology, Naya Raipur, India



ARTICLE INFO

Article history:

Received 29 March 2019

Received in revised form 6 August 2019

Accepted 25 September 2019

Keywords:

Reformed histogram equalization

Plateau limit

Krill herd optimization

Saltp swarm algorithm

Medical imaging

ABSTRACT

In this paper, a novel krill herd (KH) based optimized contrast and sharp edge enhancement framework is introduced for medical images. Plateau limit and fitness function are proposed in this paper to achieve the best-enhanced image. A new plateau limit is applied to clip the histograms using minimum, maximum, mean, and median of the histogram with a tunable parameter. The residue pixels are reallocated to the relative vacancy available on histogram bins. This method explores KH meta-heuristic algorithm to automatically adjust the tunable parameter based on a novel fitness function. Fitness function contains two different objective functions, which use edge, entropy, gray level co-occurrence matrix (GLCM) contrast, and GLCM energy of image for best visual, contrast enhancement and improved different characteristic information of the anatomical images. This method is compared with a different state of the art methods to check the viability and vigorous of the scheme and saltp swarm algorithm (SSA) optimization is also used for the fair comparison of the proposed approach. The results show that the proposed framework is having superior performance compared to all the existing methods, both qualitatively and quantitatively, in terms of contrast, information content, edge details, and structure similarity.

© 2019 Elsevier Ltd. All rights reserved.

1. Introduction

Medical imaging plays a vital role to examine the health condition of a patient and provides an effective treatment. Medical images are used for the treatment and diagnosis of a large number of diseases [1], but these images are complex in nature due to the presence of several overlapped objects in the image, which makes it difficult for the diagnostic process. Medical images, such as magnetic resonance imaging (MRI), X-ray, mammographic, and computerized tomography (CT) images, do not carry enough features for an accurate diagnosis due to low lighting conditions, environmental noises, technical restrictions of imaging devices, etc. Therefore, medical images have low quality and contrast. Contrast collectively deals with the pixel intensity differences between structures and distinct objects in the image. Region of interest (ROI) [2] or an object can be easily observed in a good contrast image.

Numerous image enhancement methods have been proposed so far in the literature for contrast and quality enhancement of the medical images. Some of them are histogram equalization, gamma

correction, and transform based approaches which have been widely used for improving the features, contrast and visual perception of both medical and natural images. Histogram equalization (HE) based algorithms are extensively used for contrast enhancement because of their effectiveness and simpler implementation. Global histogram equalization (GHE) technique generates serious constraints such as visual artifacts, noise amplification, level saturation effect, under and over-enhancement, which are not acceptable in medical imaging. Several HE-based frameworks have been emerged based on different mechanisms to overcome these limitations of the GHE. Sub-histogram, histogram clipping, and dynamic histogram equalization are the basic mechanisms that have been utilized by authors [3–7] to enhance the image's qualities and contrast.

Joseph et al. [8] introduced a fully customized enhancement framework for medical images where an arbitrary clip-limit is exploited for the clipping process, but it is tedious to set a threshold value. In anatomical images, local details can be more significant than global contrast, but local enhancement (LE) frameworks generate undesired artifacts, block effects, and also increase computational complexity. To enhance the fidelity features and contrast of the images, adaptive histogram equalization (AHE) technique [9] divides the image into small blocks and improve the pixel values of each block based on the several operations. All enhanced blocks are

* Corresponding author.

E-mail addresses: pankaj.kandhway@gmail.com (P. Kandhway), bhandari.iiitj@gmail.com (A.K. Bhandari), anurag2685@gmail.com (A. Singh).

combined to generate an enhanced image and some of LE methods are incorporated interpolation operation to remove block artifacts such as CLAHE. Contrast limited adaptive histogram equalization (CLAHE) approach is widely exploited for contrast enhancement but it is not appropriate for medical images [10,11]. An adaptive image enhancement technique was proposed by Kim [12], which basically employs a weighted gradient to improve the features of mammographic images. A new gray-level information histogram was generated in [13] for the X-ray and natural images with the help of the intensities of gradients of the equal-sized regions.

Zhao et al. [14] designed a framework to enhance the X-ray images, MRI images and CT images based on the luminance-level modulation and gradient modulation. Gandhamal [15] introduced a technique where gray-scale S-curve transformation [16] is used for medical images. Here, contrast enhancement is achieved by increasing the difference between the minimum and maximum intensity levels in the medical image. Singular value decomposition (SVD) is another image equalization method [17] where the SVD domain is created from the spatial domain and the enhanced image is generated by normalized singular value matrix. So, this technique is also called as singular value equalization (SVE) approach. In transform domain methods, image is first converted into a transform domain and then some operations are performed in this domain in order to enhance visual and contrast of the image. Further, by using inverse transformation, the enhanced image is reconstructed into a spatial domain. Wavelet-based enhancement approaches have also proposed in the literature [18–20]. Yang et al. [18] proposed a method where discrete wavelet transform (DWT) and soft thresholding schemes are used to enhance the medical images. The DWT based methods concentrate on low sub-bands of the wavelet coefficients, which contain most of the image information. But these methods do not deal with edges of the image. Edge information is a very important and useful feature for the medical image enhancement applications.

Demirel presented a framework for satellite images [19], where contrast enhancement is achieved using SVD and DWT method. Recently, Kallel et al. [20] designed an approach for poor contrast CT scans images based on adaptive gamma correction (AGC) [21] and DWT-SVD. Gamma correction based contrast enhancement methods have been utilized for natural and satellite images [21–24], but these methods have not achieved good visual results for medical images. Bhandari et al. [25] utilized DWT-SVD method coupled with cuckoo search (CS) algorithm for image contrast and brightness enhancement. In recent times, meta-heuristic optimization algorithms [26–30] have been explored for improving medical images [31,32] by tuning the parameters randomly according to the fitness or objective function. Bat algorithm was applied for the MR image enhancement by Singh [33], which maximizes the multi-objective functions such as mean opinion score and contrast enhancement factor by a modified neuron model based stochastic resonance scheme. Daniel et al. [31] introduced optimal wavelet [34,35] based masking for medical images where enhanced CS algorithm is utilized to get optimal scale value for contrast enhancement.

In this paper, a novel krill herd (KH) based image enhancement algorithm is proposed for medical images. The proposed approach cuts off its peaks which are greater than proposed plateau limit, and reforms a new histogram based on the reallocation process of clipped or residue pixels. After the generation of the reformed histogram, GHE approach is used to enhance medical images. Optimum plateau limit is generated with the help of optimization technique which is based on again a novel fitness function where krill herd and salp swarm optimization techniques are explored to find the tunable parameter. Salp swarm algorithm (SSA) [28] is a new optimization technique which follows the swarming behavior of salps when navigating and foraging in oceans.

The rest of the paper is organized as follows. In Section 2, constraints of the medical images and motivation are discussed. Section 3 represents proposed KH-RHE method for medical image. Section 4 discusses the experimental setup, results, and comparisons. Finally, the conclusion is discussed in Section 5.

2. Constraints of the medical images and Motivation

2.1. Constraints of the medical images

In general, magnetic resonance imaging (MRI) and mammogram images are employed for lower density tissues, while X-ray images [36,37] are commonly used for high-density tissues like bones. Because of the restrictions of several factors such as inherent properties and system cost of the medical imaging, the generated medical image always has the properties of inadequate brightness, low contrast, and complex noise. So, image enhancement becomes a very practical and essential means to enhance image quality, which increases the efficiency and accuracy in real-time medical applications.

Commonly, X-ray images are of low contrast. The reduced visibility of the small elements in the X-ray images is due to high X-ray penetration, blurring, scattered radiations, and the limited capacity of films, which prevent it to generate the maximum contrast. Cephalometric images of the skull containing soft tissue and bony structure details get affected from blurring due to patient moment and nonparallel radiations. The feature of X-ray images is influenced by other characteristics while capturing. In general, anatomical regions of gradual variation lead to blurring of edges. X-ray images also suffer from noise due to changes from light to photons and add noise during digitizing of films.

A mammographic image has a narrow range of gray-scale while high contrast mammogram images easily distinguish its diagnostic features, micro calcifications, and masses, from each other in comparison to the surrounding breast tissues. Mammographic images are used to detect breast cancer, which is the most frequently identified disease in women over the age of 55 years. Both cancerous and non-cancerous breast masses appear as white portions in mammogram images. The fatty tissues occur as black portions. The other parts of the breast like tumors, connective-tissue, glands, and calcium deposits appear as shades of gray, more toward the brighter gray-scale on mammogram images. The complex nature and variation of intensity level make these images as challenging to interpret diseases. Cancers can be missed and also non-cancerous lesions may be misinterpreted due to low contrast nature of mammogram image. This is the reason, radiologists fail to identify 10–30% of breast cancer cases [7]. So, high contrast, uniform texture [38,39] and sharp edges of the medical images are necessary for early and easy detection or diagnosis of breast cancer.

An MRI image is exploited for diagnosing disorder or lesions in the brain. It offers more detail information about human soft tissue framework. This image is used to detect the edema in soft tissues and acute pathologies such as cellular tumor and ischemic stroke. The MRI image [40,41] is made due to the effect of fluid and recognizes the subtle deviations at the periphery of the hemispheres and in the periventricular portion near to cerebrospinal fluid. This image has low contrast and poor readability for the diagnosis of the diseases. Computed tomography (CT) image presents better imaging of hard tissues and bones. This image contains highly imbalance between foreground voxels such as vessels, organs, etc. and background. CT scan image [42] suffers from inaccurate edges between vessels and smaller organs like gallbladder or pancreas. CT scan image has low contrast and is inappropriate in illustrating anatomy, pathology, and more truculent diagnostic checks. Multiple takes of CT scans are hurtful or even deadly sometimes for some patients due to the occurrence of anaphylaxis.

2.2. Motivation

Poor representation of information in the medical images while capturing by several devices may lead to an inaccurate diagnosis about the patient's health condition. The medical images are generally captured by exposing electromagnetic (EM) waves into the human body and recollecting the response. As EM waves are very harmful to the human tissue, it is not preferred to capture the multiple images. Actually, anatomical (medical) images have low contrast with too dark or too bright regions, different modality shows different characteristic information of diseased tissue and human viscera. Generally, medical images like MRI, X-ray images, etc. have a large background region that introduces offset intensity artifact (OIA) effect in the enhanced image. Designed an image enhancement approach which helps to avoid retakes and multiple exposures of the patients may help avoid cancer. In this paper, a novel optimized contrast enhancement framework is proposed for medical images for the preservation of sharp edges and texture features of medical images. Krill herd optimization is used for optimizing the tunable parameter based on a novel fitness function. The main contribution of the proposed framework to enhance the medical images includes simple and easy implementation of general clipping process with histogram equalization approach. It automatically adjusts the plateau limit for histogram clipping according to the nature of the image. The proposed method performance is not dependent on a particular image because its fitness function is related to the edges, energy, entropy, and contrast of the medical image.

3. Proposed method

The main contribution of this framework is the clipping limit, which is achieved by optimization algorithms such as SSA and KH based on a proposed fitness function for the medical images. The complete framework of the proposed optimization-based reformed histogram equalization is presented in Fig. 1.

3.1. Reformed histogram equalization

In the GHE [3] approach, the enhanced image is generated mainly in three steps. First, the probability density function (PDF) of each gray-scale level of the original image. After that cumulative density function (CDF) is generated using PDF and finally, transfer function (TF) is calculated using Eqs. (1) and (2)

$$T(l) = (L - 1)c(l), \text{ where } c(l) = \sum_{j=0}^l p(j) \quad (1)$$

$$p(l) = \frac{n_l}{W \times H}, \text{ where } l = 0, 1, 2, \dots, L - 1 \quad (2)$$

where $p(l)$, $c(l)$, and $T(l)$ represent PDF, CDF, and TF of the input image, respectively. The value of L is 2^8 for the 8-bit image. A number of pixels at specific intensity value l is represented as n_l . A total number of pixels or size of the image is $W \times H$. Global HE emphasizes the domination of histogram bins having a large number of pixels. Histogram bins having less number of pixels tend to be phagocytized by dominance bins in the neighborhood. The abruptly dark background of the input medical image changes to significantly larger gray levels in GHE enhanced image due to OIA. The offset intensity (OI) is occurred due to $p(0) > 0$, that means dynamic range of gray level of GHE enhanced image is $p(0) \times (L - 1)$ to $L - 1$ instead of the entire dynamic range (0 to $L - 1$).

In the case of proposed reformed histogram equalization (RHE) framework, two mechanisms are included which are clipping and reallocation operations of the histogram. Clipping process is mainly

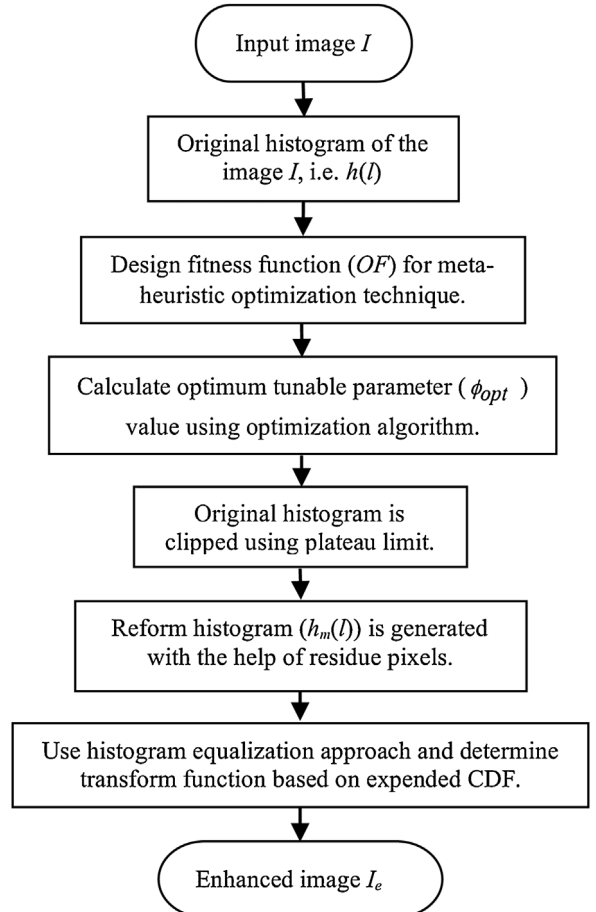


Fig. 1. Flowchart of the proposed optimization-based RHE framework.

used to control over and unnatural enhancement. Reallocation operation is used to explore the complete dynamic range where residue pixels are reallocated to the relative vacant histogram bins. Therefore, the plateau limit is the most important part of the proposed method, where a unique threshold value (plateau limit) is designed to control over-enhancement.

$$th = h(l)_{\max} - h(l)_{\min} + \phi \times abs(h(l)_{\text{mean}} - h(l)_{\text{med}}), \\ \text{where } \phi \in (0, 1) \quad (3)$$

Where $h(l)_{\min}$, $h(l)_{\max}$, $h(l)_{\text{med}}$, and $h(l)_{\text{mean}}$ represent minimum, maximum, median and mean value of the histogram, respectively. Given ϕ denotes a tunable parameter and it varies according to features of the image. The optimum value of the tunable parameter (ϕ_{opt}) is determined by using a meta-heuristic algorithm which is based on a fitness function. Clipping process is written as:

$$h_c(l) = \begin{cases} th & \text{if } h(l) \geq th \\ h(l) & \text{otherwise} \end{cases} \quad (4)$$

$$h_r(l) = \sum_{l=0}^{L-1} residue(l), \text{ where } residue(l) = (h(l) - h_c(l)) \quad (5)$$

where $h_c(l)$ and $residue$ represent clipped and residue histogram of the image, respectively, and total residue histogram or a total number of clipped pixels is denoted as $h_r(l)$. The vacancy available in the l th bin of $h_c(l)$ is represented as

$$V(l) = th - h_c(l) \quad (6)$$

when $h_c(l) = th$, $V(l) = 0$ and no vacancy is available in the l^{th} bin. The relative vacancy (RV) available in the l^{th} bin is obtained using Eq. (7)

$$RV(l) = \frac{V(l)}{\sum_{l=0}^{L-1} V(l)} \quad (7)$$

The reformed histogram is generated using $h_c(l)$, $h_r(l)$, and $RV(l)$ of the input histogram, respectively, given by:

$$h_m(l) = h_c(l) + h_r(l) \times RV(l) \quad (8)$$

Therefore, the area under modified histogram becomes equal to that of the original histogram, i.e.,

$$\sum_{l=0}^{L-1} h_m(l) = \sum_{l=0}^{L-1} h(l) \quad (9)$$

The redistribution of residue pixels in the modified histogram is a beneficial operation to stretch the contrast or dynamic intensity range, while modified histogram increases the information content of the medical image. It contributes to the preservation of naturalness of the medical image and also used as a measurable entity to access the feature of enhancement.

$$p_m(l) = \frac{h_m(l)}{W \times H} \quad (10)$$

$$c_m(l) = \sum_{j=0}^l p_m(j) \quad (11)$$

The PDF and CDF of the modified histogram are calculated using Eqs. (10) and (11), respectively. Medical images contain a significantly large dark background portion. So, $p_m(0)$ is much greater than zero and offset intensity artifact effect may occur in the enhanced image. Therefore, expanded CDF is designed where weighting cumulative distribution function is used to remove the OIA effect in the enhanced image.

$$c_e(l) = \max(c_m(l)) \left(\frac{c_m(l) - \min(c_m(l))}{\max(c_m(l)) - \min(c_m(l))} \right) \quad (12)$$

where $c_e(l)$ represents expanded CDF. After, calculation of the expanded CDF, TF or contrast enhanced intensity is computed using Eq. (13) as follows:

$$T_e(l) = (L - 1)c_e(l) \quad (13)$$

The main concept of the RHE method for medical image enhancement is that they control the over-enhancement by histogram clipping mechanism based on a plateau limit and also redistribute clipped pixels. This plateau limit is not fixed and crisp, it changes according to the features of the medical images.

3.2. Fitness function

In this paper, a new fitness function is proposed for finding the optimum value of the tunable parameter using a meta-heuristic optimization technique. A fitness function is a mathematical expression to compute how close the best solution is in finding the desired goals. The proposed framework for medical image enhancement creates a fitness criterion which is related to the edge information, entropy, gray level co-occurrence matrix (GLCM) contrast, and GLCM energy of the enhanced medical image. For the optimization problem, an objective function is required without human intervention, which can show the level of enhancement of an image automatically. For the enhancement criterion, various objective functions can be proposed considering entropy, peak signal to noise ratio and other quality parameters.

The proposed fitness function is defined in two parts where one part basically incorporates on the edge details and another part deals with the texture details of the medical image. Entropy of the image is related to the average information content and edges information is also very important in medical images. For edge detection, various techniques can be utilized such as Sobel edge detection and Canny edge detection. Sobel operator is considered to be extremely reliable and a virtuous choice for quantifying and distinguishing the edge details in the processed image compared to Laplacian and Canny edge detection operators. It is also helpful to find relevant edge information content. One of the basic requirements of the enhanced image is to have a greater number of edge pixels with higher intensity values than the original image [43]. Using the above measures together, the fitness function is defined as

$$OF1(\phi_l, \phi_u) = (\log(\log(E(I_S)))) \frac{n_{edges}(I_S)}{W \times H} H(I_e) \quad (14)$$

$$H(I_e) = - \sum_{\forall l} p_e(l) \log(p_e(l)) \quad (15)$$

where I_e is the enhanced image and I_S is Sobel edge image of the enhanced image. $\phi_l = 0$ and $\phi_u = 1$ are the minimum and maximum range of the tunable parameter, respectively. Sobel edge detection is employed in this paper for better feature preservation scheme. $E(I_S)$ is the sum of intensity values of edge pixels of image and n_{edges} is a number of such edge pixels which have intensity value greater than some fixed intensity value. $H(I_e)$ is the entropy of the enhanced image where $p_e(l)$ is the PDF of the enhanced medical image.

The gray level co-occurrence matrix is a statistical approach of examining texture where the spatial relationship of pixels is considered. In GLCM, the texture is specified by computing how often pairs of the pixel with definite values and in a particular spatial relationship exist in a medical image. Energy and contrast parameters are considered [44] to develop fitness function from 18 various parameters of GLCM. Contrast is defined as the local variations of intensity levels, high contrast is observed when large adjacent gray scale level differences occur. Energy is specified as the uniformity and it reflects pixel-pair repetitions. The co-occurrence matrix is generated in the horizontal and vertical directions and the element of the $(x, y)^{th}$ entry of this matrix is expressed as:

$$g(x, y) = \sum_{x=0}^{W-1} \sum_{y=0}^{H-1} \delta(w, h) \quad (16)$$

where

$$\delta(w, h) = \begin{cases} 1 & \text{if } I_e(w, h) = x \text{ and } I_e(w, h+1) = y \\ & \text{and } I_e(w, h) = x \text{ and } I_e(w+1, h) = y \\ 0 & \text{Otherwise} \end{cases} \quad (17)$$

where (w, h) represents the spatial coordinates of a pixel in the enhanced image and the GLCM contrast and energy is defined as:

$$I_{contrast} = \sum_{x,y} |x - y|^2 cg(x, y) \quad (18)$$

$$I_{energy} = \sum_{x,y} cg(x, y)^2 \quad (19)$$

where

$$cg(x, y) = g(x, y) / \sum_{x=0}^{W-1} \sum_{y=0}^{H-1} g(x, y) \quad (20)$$

$$OF2(\phi_l, \phi_u) = \log \left\{ I_{contrast} \times \exp(H(I_e)) I_{energy} \right\} \quad (21)$$

$$OF(\phi_l, \phi_u) = OF1(\phi_l, \phi_u) + OF2(\phi_l, \phi_u) \quad (22)$$

$$\phi_{opt} = \arg[\max\{OF(\phi_l, \phi_u)\}] \quad (23)$$

The proposed fitness function is a combination of two objective functions where edge details, entropy, and texture features are used for the best enhanced image.

3.3. Krill herd optimization technique

In the proposed framework, the krill herd optimization algorithm is exploited to achieve an optimized value of the tunable parameter by maximizing or minimizing the fitness function. Krill herd (KH) is a biologically-inspired approach by Gandomi [29] for finding the optimum solution for any complex optimization constraints where the fitness function is used to determine the distance of each krill from highest density of the swarm and food. Several studies have revealed the distribution and ecology of krill, and also krill swarm's formation. The krill density is reduced due to attack by predators such that penguins, seals, and seabirds. The reorganization of krill herd after predation is based on numerous parameters, individual krill searches and moves to find the best solution for the food and highest density.

3.3.1. Lagrangian scheme of the krill herding

This model is briefly discussed in this section, individual krill moves due to predators attack, so krill density and distance of krill from the food position is changed. This process is considered as the initial phase of KH approach. Movement induced by other krill individuals, random diffusion, and foraging activity is three basic actions considered to find the time-dependent position of an individual krill. Lagrangian model is generalized to an n-dimensional decision space

$$\frac{dY_j}{dt} = O_j + P_j + Q_j \quad (24)$$

Where, O_j , P_j , and Q_j are symbolized other krill individual motion, foraging motion, and physical diffusion of the j -th krill individuals, respectively.

3.3.1.1. Movement induced by other krill individuals. The krill individuals are moved toward high density due to their mutual effects where movement is expressed using Eq. (25). The direction of krill individuals motion induced, α_j is based on three densities which are a target swarm, local swarm, and a repulsive swarm density.

$$O_j^{new} = O_j^{max} \alpha_j + \omega_n O_j^{old} \quad (25)$$

$$\alpha_j = \alpha_j^{\text{local}} + \alpha_j^{\text{target}} \quad (26)$$

where O^{max} , ω_n , and O^{old}_j are symbolized for maximum motion induced, inertia weight, and last induced speed, respectively. α_j is a combination of the local effect (α_j^{local}) due to neighbors and target direction effect (α_j^{target}) for best krill individual. An attractive or repulsive effect of the krill neighbors is considered for a local search, krill movement individual for the neighbor's effect is determined as:

$$\alpha_j^{\text{local}} = \sum_{i=1}^M \hat{C}_{j,i} \hat{Y}_{j,i} \quad (27)$$

where $C_{j,i}$ represents fitness value of the j th krill individual for i th ($i = 1, 2, \dots, M$) neighbor and $Y_{j,i}$ denotes the related location of $C_{j,i}$. The global optima are observed where the best (lowest) fitness on j th individual krill is considered and expressed as:

$$\alpha_j^{\text{target}} = E^{best} \hat{C}_{j,best} \hat{Y}_{j,best} \quad (28)$$

where E^{best} denotes an effective coefficient for the best fitness on j th krill individual.

3.3.1.2. Foraging motion. Food location and prior knowledge about the food location are two factors to determine the foraging motion for j th krill individual. Foraging motion is written as:

$$P_j = V_f \beta_j + w_f P_j^{old} \quad (29)$$

$$\beta_j = \beta_j^{food} + \beta_j^{best} \quad (30)$$

where w_f denotes inertia weight of the foraging speed and V_f is the foraging speed. Food attractive (β_j^{food}) is specified to perhaps attract the krill swarm to the global optima, and the best objective of the j th krill is denoted as β_j^{best} .

3.3.1.3. Physical diffusion. It is a random process for krill individuals where motion is expressed in terms of a random directional vector (δ) and a maximum diffusion speed (Q^{max}). The less random motion indicates the optimal position of the krill.

$$Q_j = Q^{max} \delta \quad (31)$$

3.3.1.4. Motion process of the KH algorithm. From the above discussion, it is clear that a better objective function is more important to find the movement of the j th krill individual. A random search is used to generate the best solution, the position of the krill during the interval t to $t + \Delta t$ is expressed in Eq. (32)

$$Y_j(t + \Delta t) = Y_j(t) + \Delta t \frac{dY_j}{dt} \quad (32)$$

$$\Delta t = E_t \sum_{k=1}^{MV} (U_k - L_k) \quad (33)$$

where Δt depends on the search space, E_t is a constant parameter, MV denotes the total number of variables, and L_k and U_k represent lower and upper bounds of the k th variables, respectively.

3.3.2. Genetic operations

In KH algorithm, crossover and mutation mechanisms are incorporated to improve performance, genetic reproduction mechanisms are considered from classical differential evolution techniques.

3.3.2.1. Crossover. It is an effective strategy used for global optimization and considered as a further development to genetic algorithm. An adaptive vectorized crossover is controlled by a probability where crossover probability (Cp) increases with decreasing the objective.

$$y_{j,m} = \begin{cases} y_{r,m} & \text{rand}_{j,m} < Cp \\ y_{i,m} & \text{else} \end{cases} \quad (34)$$

where $y_{r,m}$ is the m th component of the Y_j and $r \in \{1, 2, \dots, M\}$, M denotes the number of the krill individuals.

3.3.2.2. Mutation. Adaptive mutation operation is explored where mutation probability (Mu) is used to find the global optimization and it also increases with the fitness.

$$y_{j,m} = \begin{cases} y_{gbest,m} + \mu(y_{p,m} - y_{q,m}) & \text{rand}_{j,m} < Mu \\ y_{i,m} & \text{else} \end{cases} \quad (35)$$

where μ is a constant parameter and $p, q \in \{1, 2, \dots, Y\}$.

In this optimization technique, two local and two global schemes work in parallel which produces notable and efficient

Table 1

Parameters and values used for optimization techniques.

Algorithms	Parameters	Values
SSA [28]	Swarm size	15
	No. of iteration	100
	Lower and upper bound	0 and 1
KH [29]	Crossover flag	1
	No. of iteration	100
	Lower and upper bound	0 and 1
	Krill size	15
	Runs	1

results. It is also able to generate global minima for all type of constraints with a high degree of accuracy. The maximum value of the fitness function is obtained by minimizing the negative value of the fitness function. It is based on the stochastics random search in the place of a gradient search so, derivative information is not required for finding the optimal solution. In the case of meta-heuristic optimization techniques, tuning parameters are very important to generate the best solution. KH algorithm uses only time interval (E_t) that is fine-tuned in this algorithm, one tunable parameter of the KH approach is a remarkable advantage over other nature inspired techniques. The specific values of important parameters of KH and SSA optimization algorithms are presented in Table 1.

4. Experimental results and discussion

The performance evaluation of the proposed algorithm has been carried on the medical images obtained from a publicly available database such as MIAS, LITFL databases. These databases include various types of medical images like X-ray, MRI, and CT-scan images of different body parts. All the experiments were performed on a system having 3.1 GHz Intel Core i7 processor with 6 GB RAM. Each algorithm was run ten times and then average result was calculated. In order to demonstrate the effectiveness of the proposed algorithms, several well-known methods are compared. To compare the quantitative results of implemented algorithms with the proposed algorithms, various performance evaluation metrics are used, whose details are given in Table 2. The proposed KH-RHE and SSA-RHE frameworks are compared with other five methods which include existing well-known approaches such as GHE [3], DWT-SVD [19], AGC [21], Local S-curve [15] and DWT-SVD-AGC [20].

4.1. Qualitative evaluation

The ultimate objective of medical imaging is to diagnose/identify certain organs in the body for any abnormality. For example, X-ray images are used for identifying or locating any possible fracture in dense parts of the body such as bones. Applications

Table 2

Different metrics to test the efficiency of the approaches.

Parameters	Formula	Remarks
Structural Similarity Index (SSIM) [8]	$SSIM(I, I_e) = \frac{(2\mu_I\mu_{I_e} + C1)(2\sigma_{II_e} + C2)}{(\mu_I^2 + \mu_{I_e}^2 + C1)(\sigma_I^2 + \sigma_{I_e}^2 + C2)}$	Compares the structure of enhanced image with original image.
Edge preserve index (EPI) [45]	$EPI(I, I_e) = \frac{\sum_{x,y} I_e(x,y) - I_e(x,y+1) + I_e(x,y) - I_e(x+1,y) }{\sum_{x,y} I(x,y) - I(x,y+1) + I(x,y) - I(x+1,y) }$	Represents how efficient the salient edges in input image are preserved in the output image.
Entropy (DE) [14]	$H = - \sum_l P(l) \log(P(l))$	Quantifies the information present in the image.
Relative enhancement in contrast [14]	$REC = \frac{C_e}{C_l} \quad C_e = 20 \log \left[\frac{\frac{1}{W \times H} \sum_{w=1}^W \sum_{h=1}^H (I_e^2(x, y)) - \left(\frac{1}{W \times H} \sum_{w=1}^W \sum_{h=1}^H (I_e(x, y)) \right)^2}{\frac{1}{W \times H} \sum_{w=1}^W \sum_{h=1}^H (I_e(x, y))} \right]$	A performance metric which measures the level of contrast in an image.

include bone degeneration or disease diagnosis, fractures and dislocations identification, etc. On the other hand, CT scan images are more useful in diagnosing conditions affecting the vertebrae and other bones of the spine. MRI images provide best resolution and contrast for softer tissues and hence used for detecting brain tumor, brain tissue segmentation, bleeding or swelling detection at the tissue level. Several acquisition constraints may result these images into low-contrast images, which may severely affect their diagnostic usability. Hence, contrast enhancement in these images without altering their clinical information content is very much required for diagnostic applications. For example, in brain MRI images, contrast enhancement may result into pixel intensity difference between soft and hard tissues, which can be quite helpful in precise detection of clots/injuries in soft tissues that may otherwise go undetected. Therefore, we have taken a variety of medical images as test images and their qualitative evaluation using the proposed algorithm has been carried out. For the performance analysis in terms of contrast enhancement and edge preservation, enhancement results obtained from all the algorithms being compared and the proposed KH-RHE method with original images are depicted in Figs. 2, 4–10. A histogram plot of a particular image (Med1) for each method with original histogram is represented in Fig. 3. GHE, DWT-SVD, AGC, Local S-curve, and DWT-SVD-AGC methods generate high contrast enhanced images with respect to the original image. But these enhanced medical images do not provide adequate visual information due to invariant visual qualities. GHE shifts the intensities toward the extreme left or the extreme right region of the histogram because it stretches the contrast level of the low histogram portions and compresses the contrast level of the high histogram portions as shown in Fig. 3(b). This intensity shifting property is considered as level saturation effects. Therefore, interested in small regions of the image may not be properly enhanced as depicted in Figs. 2(b), 4(b)–10(b). Generally, DWT-SVD method generates contrast enhanced image, but some edge information is removed in low and high intensity levels. Furthermore, the low intensity range is not suitably improved using this algorithm. This technique is also suffered from offset intensity artifact as shown in Figs. 2(c), 4(c)–10(c).

AGC method produces contrast enhanced medical image but it suffers from over and under brightness conditions. To control this, it needs a careful selection of the gamma value in the algorithm. This method does not preserve edge details and also generates visually degraded images as illustrated in Figs. 2(d), 4(d)–10(d). In Local S-curve method, the medical image is divided into non-overlapping blocks and sigmoid function is applied on each block, so the complexity of the method is increased. This algorithm has reduced the visual clarity of small details due to properties of the sigmoid function and introduces blocking effects as shown in Figs. 2(e), 4(e)–10(e). The sigmoid function causes dark pixels to be even darker, and the bright pixels to be even brighter. Enhanced images

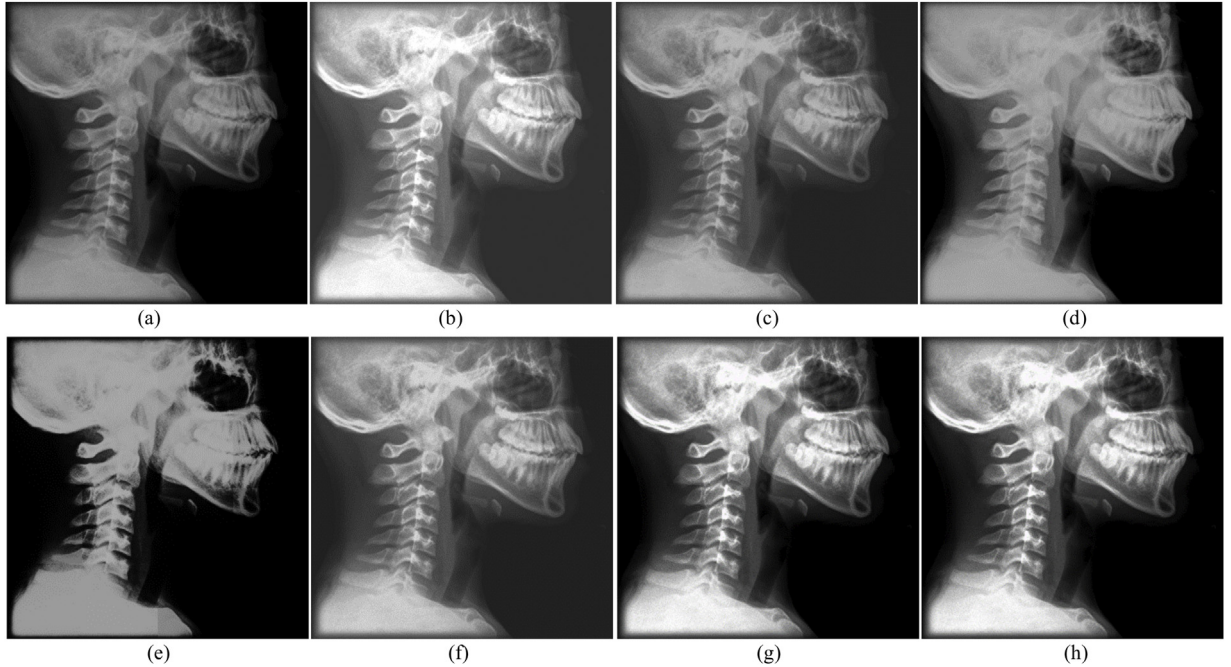


Fig. 2. Input image and the corresponding enhancement results by different methods (a) Input Med1 image, (b) HE, (c) DWT-SVD, (d) AGC, (e) Local S-curve, (f) DWT-SVD-AGC, (g) SSA-RHE, and (h) KH-RHE.

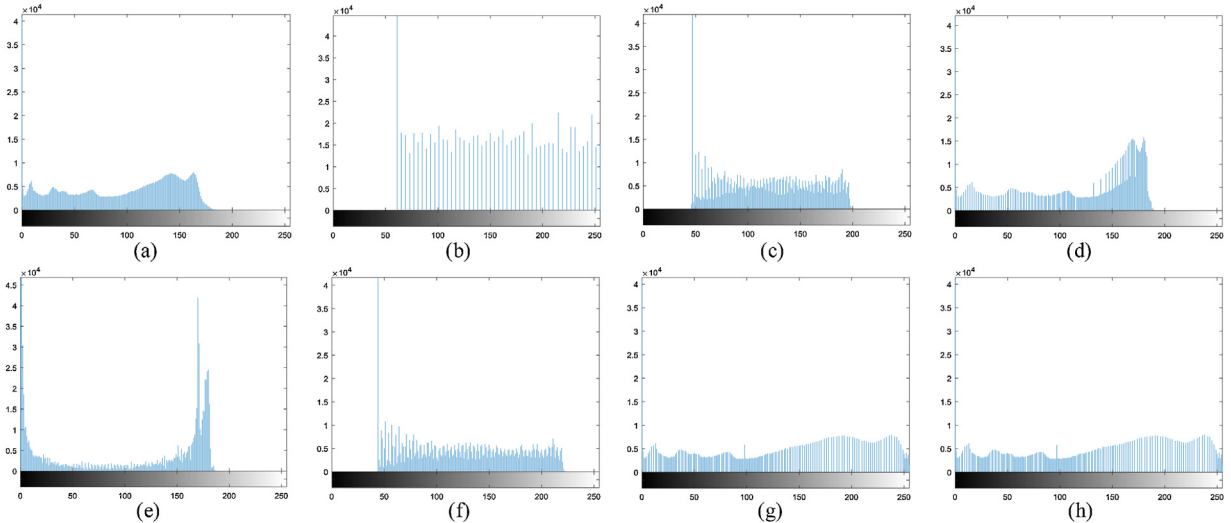


Fig. 3. (a) Histogram of the Med1 image and histogram using different methods for Med1 image, (b) HE, (c) DWT-SVD, (d) AGC, (e) Local S-curve, (f) DWT-SVD-AGC, (g) SSA-RHE, and (h) KH-RHE.

of the DWT-SVD-AGC method are depicted in Figs. 2(f), 4(f)–10(f). These images are visually degraded and also OIA is present in the enhanced images.

The original histogram has a limited dynamic range, which is extended by GHE but not completely. There exist wide gaps in the histogram that shows isolated bins. Also, the GHE approach does not maintain the shape of the histogram and leads to noise amplification. DWT-SVD and DWT-SVD-AGC methods slightly extended and shifted the histogram but these methods generate histogram peaks at the beginning of the histogram. Similarly, Local S-curve and AGC methods do not follow the shape of the original histogram. Histogram of the proposed KH-RHE and SSA-RHE covers the entire dynamic range and reduces the peaks. These histograms follow the original shape of histogram with uniformly distributed structure as presented in Fig. 3. The proposed approaches are more efficient

in terms of visual quality as shown in Figs. 2(g)–(h), 4(g)–(h) to 10(g)–(h).

The proposed KH-RHE framework generates better enhanced results in terms of contrast, edge details, details information, and texture features for X-ray images as shown in Figs. 2(h), 4(h)–5(h). Both proposed methods do not contain OIA during the enhancement process, but other methods are suffered from OIA as shown in Figs. 2–10. Generally, contrast enhancement methods are exploited as a preprocessing module which is very helpful to improve the clarity of the diagnosis. This method produces appropriate contrast image enhancement, which is visually more prominent, informative, and natural in term of preserving originality such as edge and details information can be seen in Figs. 6(h)–8(h). It controls the enhancement rate and also preserves the texture features of the image. It also increases the contrast between normal dense tis-

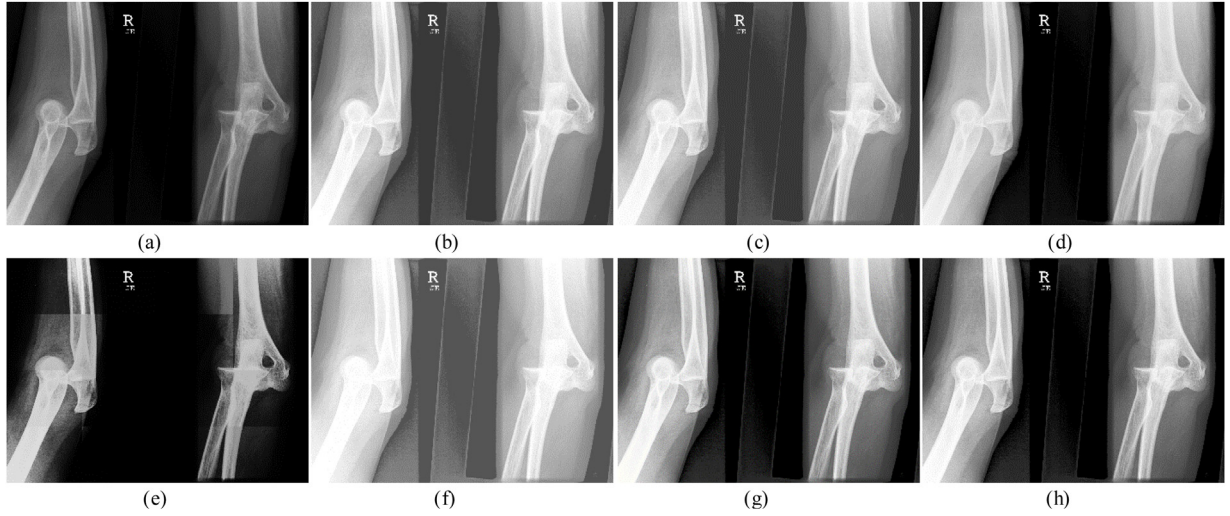


Fig. 4. (a) Input Med2 image, (b) HE, (c) DWT-SVD, (d) AGC, (e) Local S-curve, (f) DWT-SVD-AGC, (g) SSA-RHE, and (h) KH-RHE.

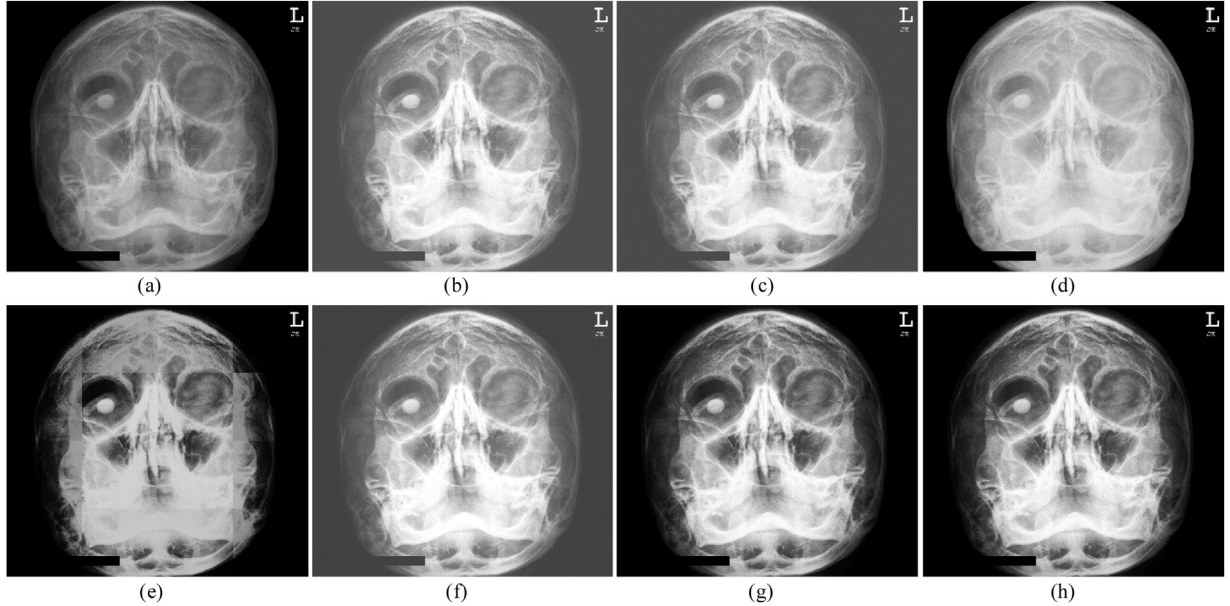


Fig. 5. (a) Input Med3 image, (b) HE, (c) DWT-SVD, (d) AGC, (e) Local S-curve, (f) DWT-SVD-AGC, (g) SSA-RHE, and (h) KH-RHE.

sue and malignant of a mammogram image. For MRI and CT scan images, again the proposed methods show the best visual results as shown in Figs. 9–10. Even the softer tissues got enhanced in these images and a good visual contrast has been achieved. A good resolution at tissue level helps in better diagnosis using MRI and CT scan images.

To demonstrate the illustrative advantages of the proposed KH-RHE method, two regions (enclosed within red boxes) of MRI and CT-scan images are selected in this paper as shown in Fig. 11. Some important areas of Med7(I), Med7(II), Med8(I), and Med8(II) images are highlighted with red arrows to show dissimilarity and fine details as depicted in Figs. 12–15. The cranial nerves and cerebral of the human brain are clearly visible and easily detectable portions in the Med7(I) and Med7(II) images enhanced by the proposed approach as shown in Figs. 12 and 13. Soft tissue boundaries and lobes are usually not well enhanced by all algorithms excluding both designed SSA-RHE and KH-RHE frameworks to detect the patient's health conditions. Longitudinal cerebral fissure and corpus callosum of the human brain is remarkably observed in KH-RHE and SSA-RHE enhanced images as compared to all well-known

techniques. Human rib, pancreas, stomach, and intestine portions indicated by red arrows are clearly visible and well enhanced by KH-RHE and SSA-RHE methods as shown in Figs. 14 and 15. Moreover, texture features and contrast of enhanced (KH-RHE and SSA-RHE) images are finest compared to all other enhanced images.

4.2. Quantitative evaluation

Quantitative analysis of the enhanced medical images is very important in comparing different enhancement methods. Besides the visual results, structure similarity index (SSIM), edge preserve index (EPI), entropy, and relative enhancement in contrast (REC) are well-known fidelity parameters, which are used for quantitative performance analysis. SSIM is used to measure structural similarity information that compares local patterns of pixel intensities that have been normalized for contrast and luminance. It may help to gauge the overall morphology preservation of the medical image. REC deals with the level of contrast which gives an idea about the pixel intensity differences between structures and distinct objects in the medical image. SSIM and REC parameters should be highest to

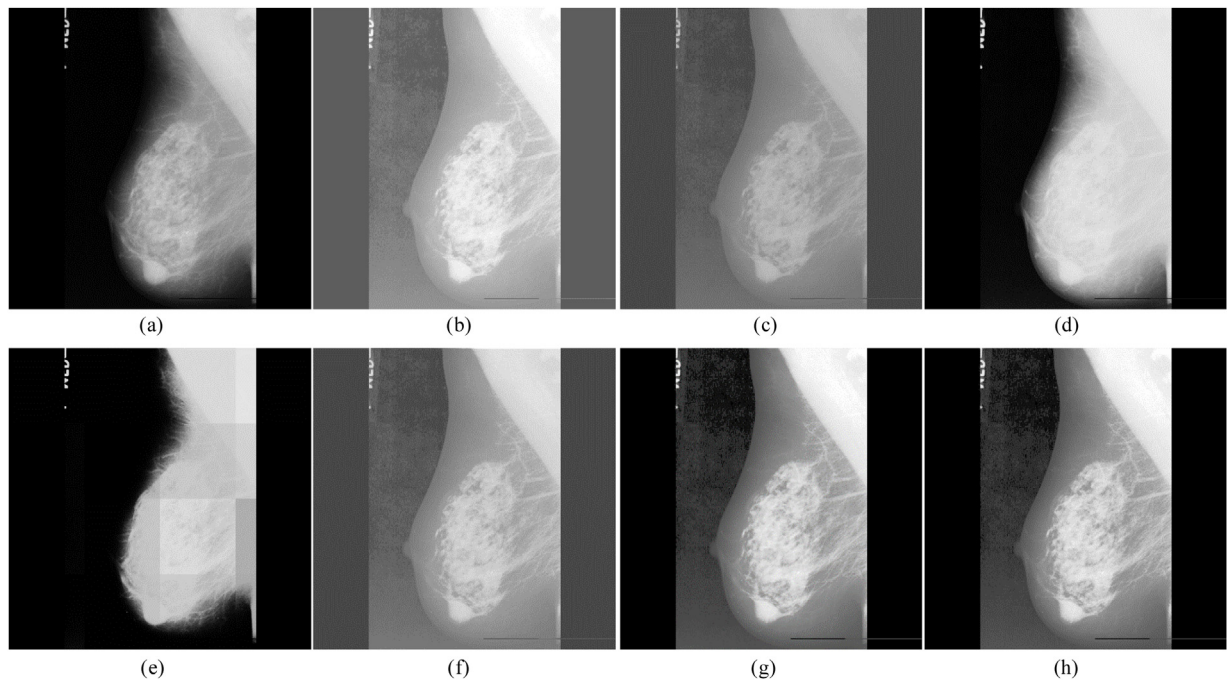


Fig. 6. (a) Input Med4 image, (b) HE, (c) DWT-SVD, (d) AGC, (e) Local S-curve, (f) DWT-SVD-AGC, (g) SSA-RHE, and (h) KH-RHE.

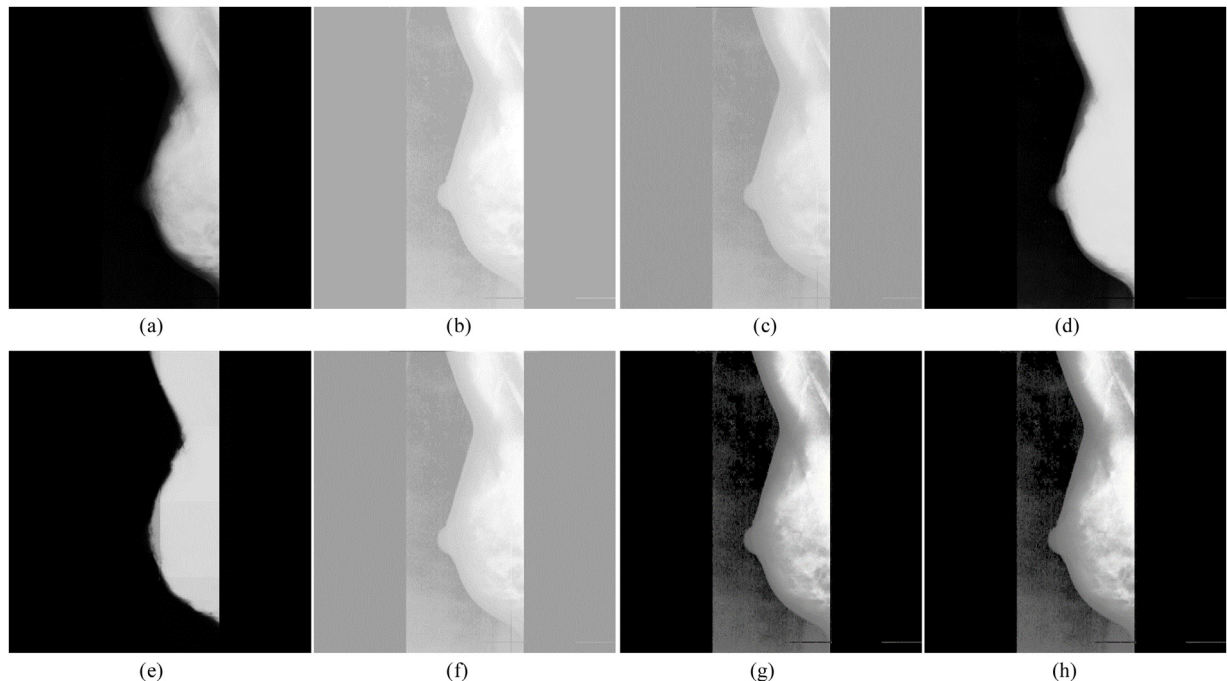


Fig. 7. (a) Input Med5 image, (b) HE, (c) DWT-SVD, (d) AGC, (e) Local S-curve, (f) DWT-SVD-AGC, (g) SSA-RHE, and (h) KH-RHE.

Table 3

Comparison of SSIM and EPI values for each method.

Image	SSIM						EPI							
	HE	DWT-SVD	AGC	Local S-curve	DWT-SVD-AGC	SSA-RHE	KH-RHE	HE	DWT-SVD	AGC	Local S-curve	DWT-SVD-AGC	SSA-RHE	KH-RHE
Med1	0.5840	0.6537	0.9332	0.7604	0.6473	0.9340	0.9350	1.2356	0.9993	0.8655	1.1871	1.1375	1.6158	1.6158
Med2	0.4925	0.5032	0.8033	0.8063	0.4227	0.8096	0.8101	1.0715	1.1323	0.9551	1.4314	0.9695	1.3627	1.3627
Med3	0.6020	0.6153	0.7037	0.8074	0.6063	0.8896	0.8907	1.1969	1.1336	0.9329	1.4376	1.1869	1.6826	1.6823
Med4	0.3554	0.3843	0.9011	0.4311	0.3795	0.8502	0.8502	1.2456	1.1835	0.8901	0.8534	1.3368	1.9127	1.9132
Med5	0.1525	0.1574	0.9180	0.8207	0.1564	0.8436	0.8437	1.0715	1.3222	1.1422	0.6999	1.4131	3.5992	3.5997
Med6	0.4228	0.3604	0.9218	0.6761	0.4110	0.8401	0.8409	1.0041	0.8644	0.9944	0.9767	1.0957	1.5384	1.5386
Med7	0.4435	0.4677	0.7770	0.5738	0.4808	0.7924	0.7928	1.4876	1.4391	1.3366	1.1715	1.5093	1.9726	1.9731
Med8	0.5258	0.5347	0.8881	0.7073	0.5458	0.9237	0.9237	0.8834	0.8930	1.0952	1.3285	0.9379	1.2608	1.2608

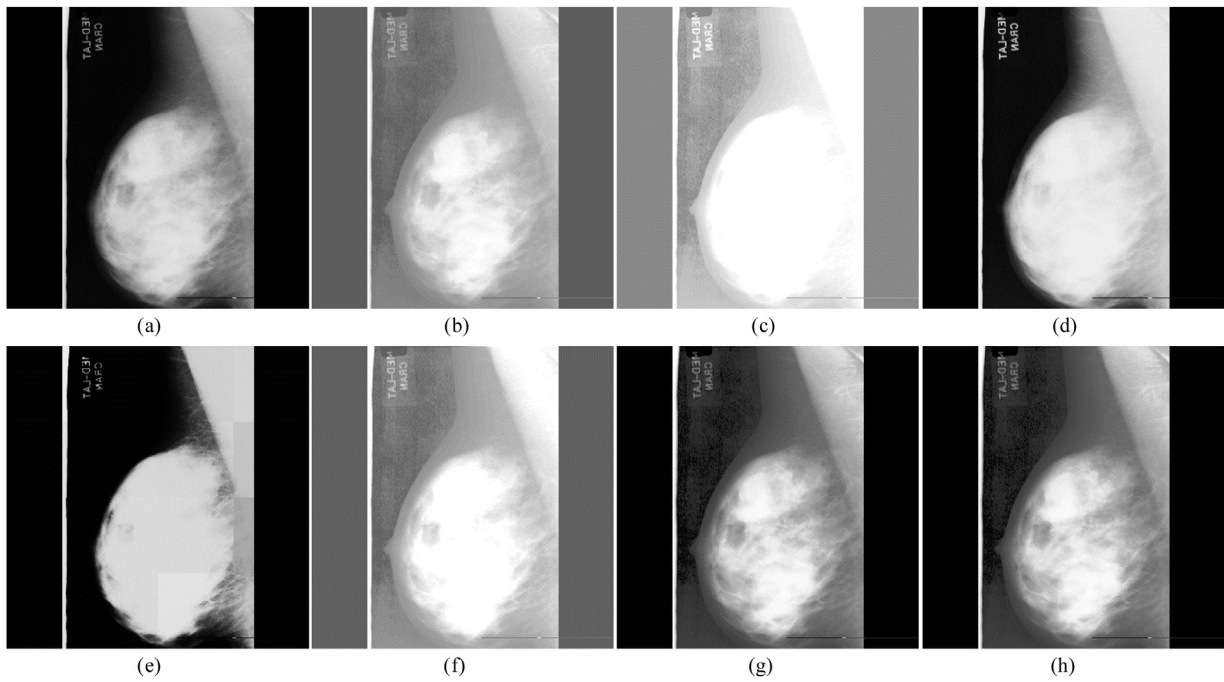


Fig. 8. (a) Input Med6 image, (b) HE, (c) DWT-SVD, (d) AGC, (e) Local S-curve, (f) DWT-SVD-AGC, (g) SSA-RHE, and (h) KH-RHE.

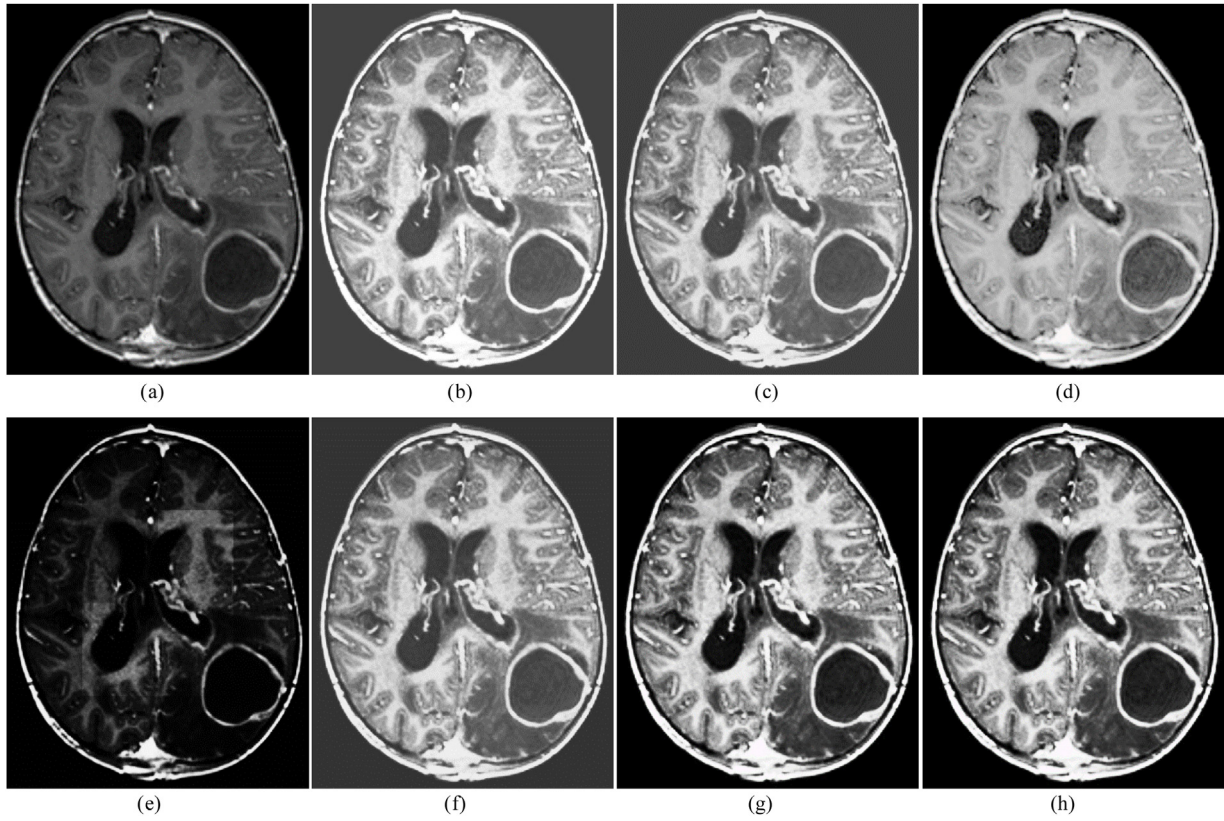


Fig. 9. (a) Input Med7 image, (b) HE, (c) DWT-SVD, (d) AGC, (e) Local S-curve, (f) DWT-SVD-AGC, (g) SSA-RHE, and (h) KH-RHE.

avoid any poverty in the structure details and for the clear visibility of the diagnostic features in the enhanced medical images. EPI and entropy are incorporated to evaluate how much salient and sharp edge details and average information is altered by the algorithm in the enhanced medical images. To ensure the retention of the clinically important image features, the values of EPI and entropy

should be highest and close to the original value, respectively. The highest values of EPI and REC indicate high edge intensity values (more diagnostic details) and better visual results (more clarity), respectively. Comparison is done here using values of SSIM, EPI, entropy, REC, fitness value (OF) and execution time of the proposed approaches with the well-known methods. The quantitative SSIM

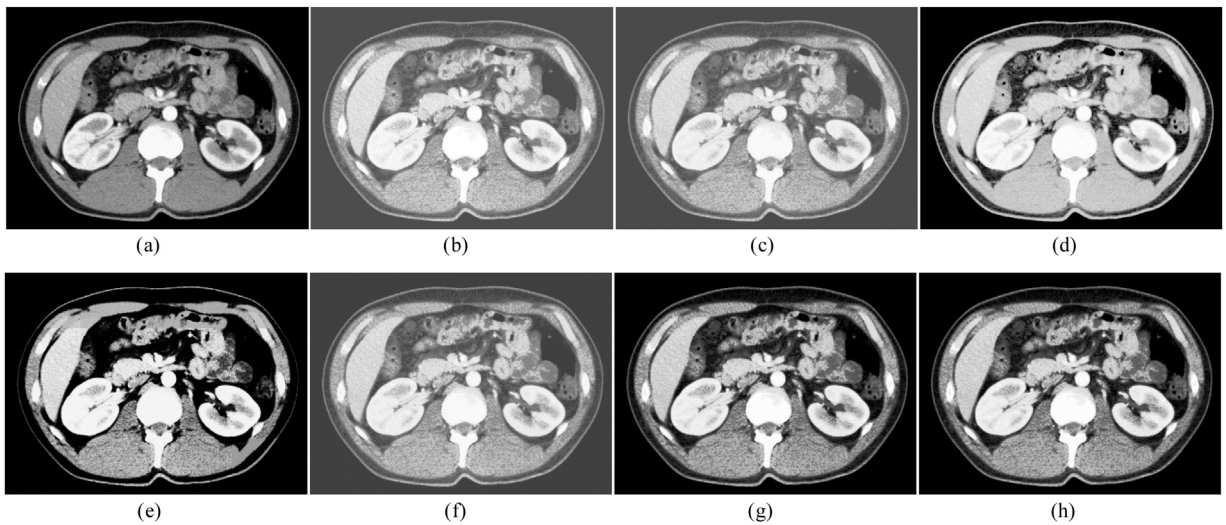


Fig. 10. (a) Input Med8 image, (b) HE, (c) DWT-SVD, (d) AGC, (e) Local S-curve, (f) DWT-SVD-AGC, (g) SSA-RHE, and (h) KH-RHE.

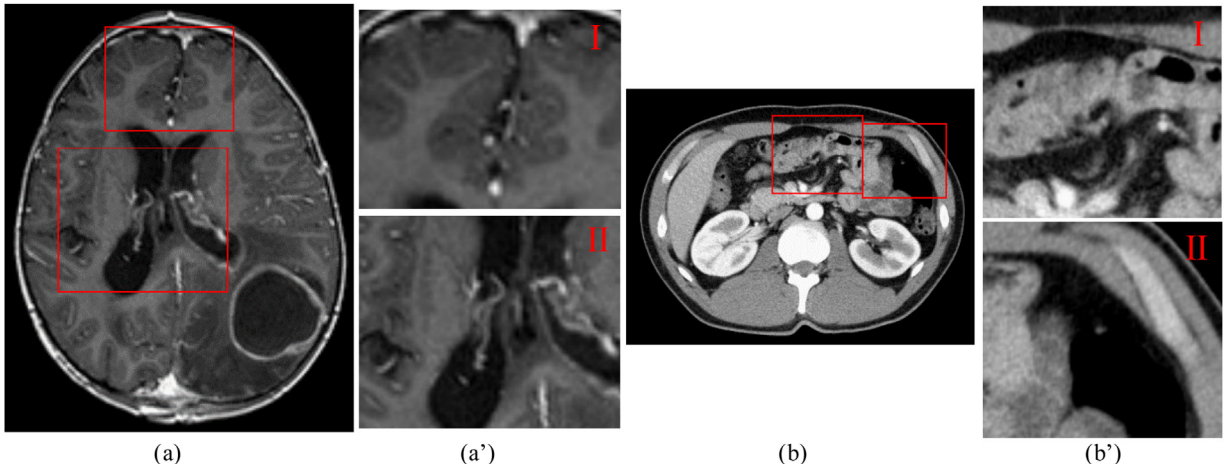


Fig. 11. (a) Input Med7 image, (a') selected I and II regions of the Med7 image, (b) Input Med8 image, and (b') selected I and II regions of the Med8 image.

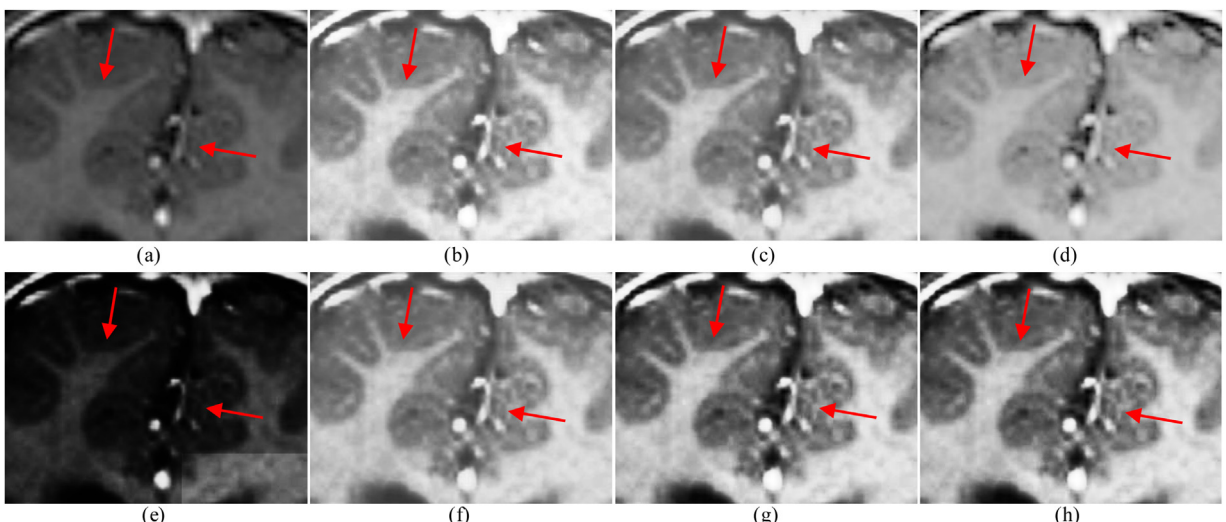


Fig. 12. (a) Input Med7 (I) image, (b) HE, (c) DWT-SVD, (d) AGC, (e) Local S-curve, (f) DWT-SVD-AGC, (g) SSA-RHE, and (h) KH-RHE.

and EPI results are presented in [Table 3](#), similarly, the measured entropy and RCE values are illustrated in [Table 4](#). [Table 5](#) presents the fitness value and execution time of the enhanced images.

The SSIM value of the proposed KH-RHE approach is highest or second highest for most of the cases, AGC method generated highest SSIM values for Med 4, Med5, and Med6 input images

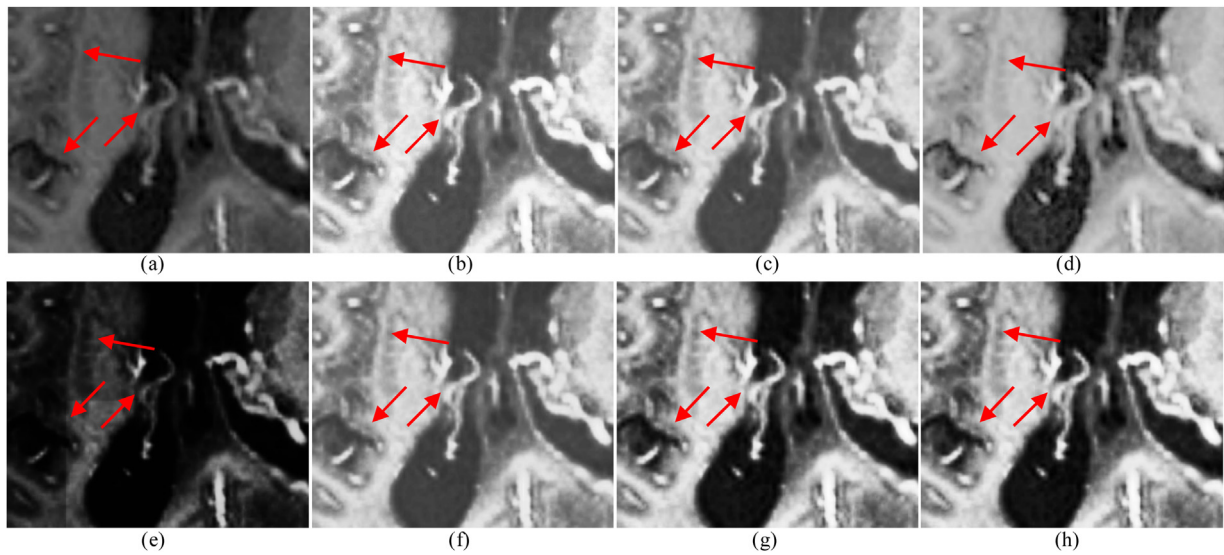


Fig. 13. (a) Input Med7 (II) image, (b) HE, (c) DWT-SVD, (d) AGC, (e) Local S-curve, (f) DWT-SVD-AGC, (g) SSA-RHE, and (h) KH-RHE.

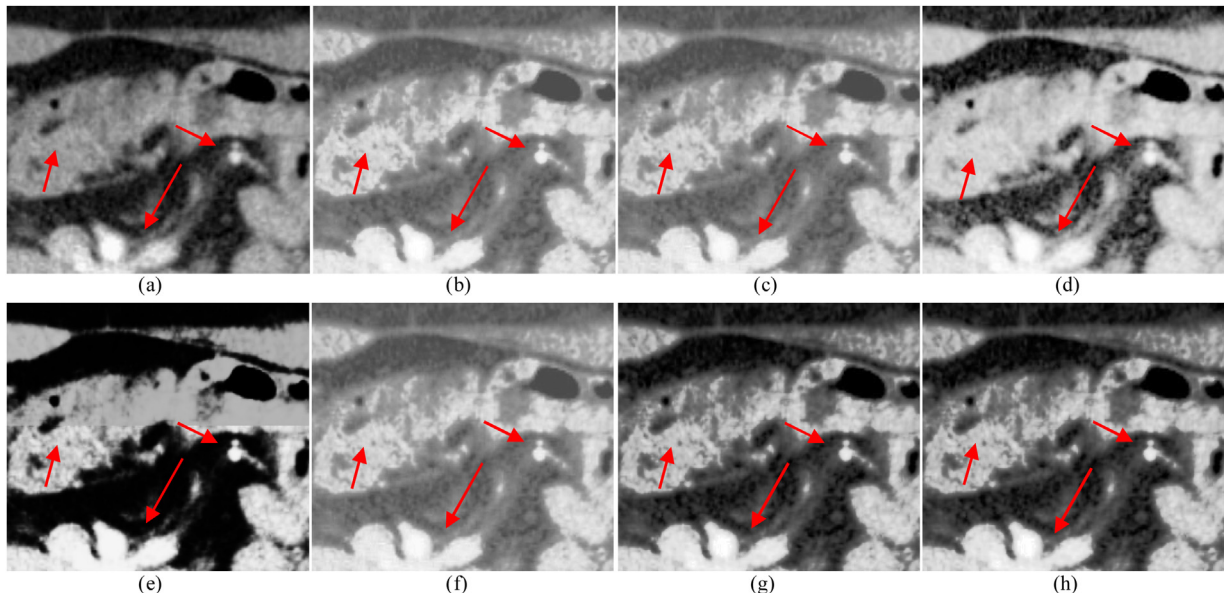


Fig. 14. (a) Input Med8 (I) image, (b) HE, (c) DWT-SVD, (d) AGC, (e) Local S-curve, (f) DWT-SVD-AGC, (g) SSA-RHE, and (h) KH-RHE.

Table 4

Comparison of entropy and REC values for each method.

Image	Entropy								REC							
	Original	HE	DWT-SVD	AGC	Local S-curve	DWT-SVD-AGC	SSA-RHE	KH-RHE	HE	DWT-SVD	AGC	Local S-curve	DWT-SVD-AGC	SSA-RHE	KH-RHE	
Med1	6.3775	4.9925	6.1907	6.0283	5.5697	6.3507	6.3541	6.3542	1.0128	0.9485	1.0361	1.0577	0.9854	1.0775	1.0775	
Med2	6.4812	5.0694	6.6572	6.2565	5.8464	6.2698	6.3462	6.3493	1.0305	1.0288	1.1037	1.0534	1.0144	1.1066	1.1071	
Med3	6.1116	4.6425	6.1033	5.8735	6.2831	6.1124	6.0201	6.0188	0.9853	0.9821	1.0575	1.0560	1.0057	1.0697	1.0695	
Med4	5.2595	4.0578	5.3132	4.8404	4.3538	5.4880	5.0596	5.0618	0.9180	0.8597	1.0514	1.0345	0.9048	1.0172	1.0164	
Med5	2.9325	2.2896	3.2223	2.4959	1.8894	3.3158	2.8256	2.8256	0.7576	0.7415	1.0076	1.0193	0.7695	1.0133	1.0132	
Med6	5.4385	4.1120	3.6166	5.0176	4.2206	4.8926	5.2718	5.2731	0.8978	0.8875	1.0388	1.0257	0.9296	0.9957	0.9956	
Med7	6.0358	4.8811	6.3784	5.9344	5.4452	6.4019	5.8708	5.8750	1.0912	1.0765	1.1517	1.0058	1.0855	1.1665	1.1665	
Med8	6.1889	4.6324	6.0640	5.8696	5.5653	6.1141	6.0000	6.0000	0.9401	0.9305	1.0478	1.0433	0.9423	1.0206	1.0206	

but this approach is inefficient in terms of visual quality and contrast enhancement as shown in Figs. 6–8. Though, SSIM is not a diagnostic measure, but its highest value indicates that the proposed approach maintains the overall morphology of the medical images in the contrast enhanced condition. The proposed KH-RHE

approach produces the highest value of EPI and REC quality parameters for more number of medical images. SSA-RHE framework also produces the second best qualitative results with respect to all the other existing methods. Edge preservation is vital for all medical image processing applications, especially involving image segmen-

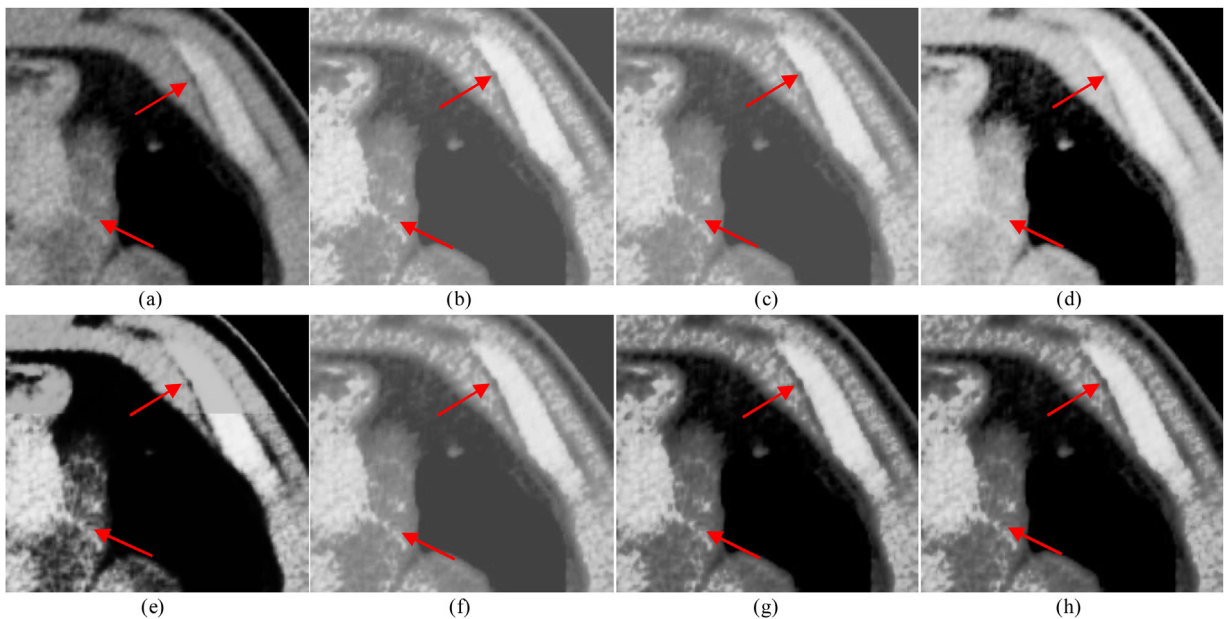


Fig. 15. (a) Input Med8 (II) image, (b) HE, (c) DWT-SVD, (d) AGC, (e) Local S-curve, (f) DWT-SVD-AGC, (g) SSA-RHE, and (h) KH-RHE.

Table 5

Comparison of values of fitness function (OF) and execution time for each method.

Image	Fitness value							Execution time (Seconds)						
	HE	DWT-SVD	AGC	Local S-curve	DWT-SVD-AGC	SSA-RHE	KH-RHE	HE	DWT-SVD	AGC	Local S-curve	DWT-SVD-AGC	SSA-RHE	KH-RHE
Med1	4.5771	5.4612	4.8481	4.3101	5.7294	6.1738	6.1740	0.0294	2.3736	1.0361	0.0396	2.4110	198.11	215.39
Med2	4.2597	5.8549	4.8635	4.7070	5.1873	5.7206	5.7251	0.0314	6.1633	1.1037	0.1232	6.3892	442.76	453.48
Med3	4.0431	5.5430	5.0131	6.0689	5.5198	6.0363	5.9850	0.0598	2.0283	1.0775	0.0436	2.1105	161.56	172.55
Med4	2.5287	3.6393	2.9677	2.1364	3.9343	4.2744	4.2924	0.0266	2.3399	1.0514	0.0417	2.3707	187.37	202.29
Med5	1.3785	0.7968	0.0784	1.1254	0.7465	1.2585	1.2610	0.0295	2.5677	1.0372	0.0427	2.3782	181.32	195.35
Med6	3.0367	1.8186	4.0509	3.0415	3.5599	4.8101	4.8414	0.0267	2.2940	1.0388	0.0410	2.5067	199.37	212.25
Med7	4.5369	6.3623	5.6376	3.8446	6.3624	6.1696	6.1734	0.0277	1.6267	1.1517	0.0527	1.7329	135.50	145.78
Med8	4.2912	5.5884	5.7355	5.4023	5.5507	6.0324	6.1136	0.0278	1.7073	1.0478	0.0368	1.7729	151.55	163.61

tation tasks such as tissue segmentation in cancer detection, brain anomaly detection (using MRI images), etc. The proposed KH-RHE and SSA-RHE frameworks maintain optimum values for EPI and REC which indicates that the designed frameworks preserve the sharp edges with proper contrast enhancement in the medical images making them suitable for diagnostic purposes.

The entropy values of the proposed methods are close to the original entropy as represented in Table 4. The enhanced medical images by DWT-SVD and DWT-SVD-AGC have entropy greater than the original value for some images. The large values indicate noise and undesired artifacts in the enhanced images that are generated during the enhancement process and thus altering their diagnostic features. So, the proposed SSA-RHE and KH-RHE frameworks outperforms the state-of-the-art methods by producing the best visual results and fidelity parameters. As the digital mammograms, MRI, and CT scans are textural images, it is necessary to preserve texture features during the enhancement process. The proposed frameworks generate the high value of fitness function that indicates the preservation of edge details, texture features, and other detail information. That means they do not add any artifacts and visual distortions during the enhancement process. The enhanced KH-RHE images have slightly more visual clarity, SSIM, information content, EPI, REC, and OF than those of enhanced SSA-RHE images. Though the run time of KH-RHE method is longer than that of the SSA-RHE method which is presented in Table 5. From the qualitative and quantitative analysis, it can be seen that comparable techniques achieve contrast and take less execution or processing

time. But, these methods do not provide high-quality images due to lower values of REC, SSIM, entropy, OF, and EPI. The enhanced medical images from the proposed KH-RHE method are better than all the comparable methods in terms of both the quantitative evaluation and visual assessment.

5. Conclusion

Image enhancement methods are the most widely used approaches for interpretation, monitoring, and diagnosis of the diseases associated with underlying tissues in the human body. The optimization based SSA-RHE and KH-RHE frameworks have been designed in this work to automatically select the plateau limit that is variant and flexible according to mammogram, MRI, CT, and X-ray images without human intervention. The automatic plateau limit is suitable for automatic systems which are generated with the help of a new fitness function. Both proposed methods handled the texture nature of medical images. These methods are more suitable for a low degree of gray level discontinuities. These methods have been found to be able to enhance the very fine details of the medical images which are very helpful to diagnosis and treatment of the disease. Clipping and reallocation processes are incorporated with GHE to control over-enhancement by restricting the enhancement rate and increases the dynamic gray level of the image, respectively. Both proposed frameworks have been found to be superior for contrast enhancement than the existing methods including GHE, AGC, Local S-curve, DWT-SVD and DWT-

SVD-AGC. These existing approaches suffer with the presence of histogram spikes, offset intensity artifact, degraded visual quality, and inefficient contrast in the enhanced images. The proposed KH-RHE and SSA-RHE approaches to overcome the OIA and follow the shape of the original histogram. The histograms of the proposed enhanced images spread more over the full range of gray-scale, so there is no saturation and washed-out appearance in the output images. These methods also take more execution time for all images which is measured as a computational time of each method. However, the proposed KH-RHE framework is the slowest among all methods but, it generates best results among all the comparable methods followed by SSA-RHE in terms of qualitative and quantitative aspects. So, both introduced KH-RHE and SSA-RHE methods are more appropriate for low contrast medical images to treatment and diagnosis of the disease.

Declaration of Competing Interest

We have no conflict of interest to declare.

References

- [1] Jose Juan Garcia-Hernandez, Wilfrido Gomez-Flores, Javier Rubio-Loyola, Analysis of the impact of digital watermarking on computer-aided diagnosis in medical imaging, *Comput. Biol. Med.* 68 (2016) 37–48.
- [2] Sebastian Schäfer, Kim Nylund, Fredrik Sevik, Trond Engjom, Martin Mézl, Radovan Jiřík, Georg Dimcevski, Odd Helge Gilja, Klaus Tönnies, Semi-automatic motion compensation of contrast-enhanced ultrasound images from abdominal organs for perfusion analysis, *Comput. Biol. Med.* 63 (2015) 229–237.
- [3] Yeong-Taeg Kim, Contrast enhancement using brightness preserving bi-histogram equalization, *IEEE Trans. Consum. Electron.* 43 (1) (1997) 1–8.
- [4] Soong-Der Chen, Abd Rahman Ramli, Minimum mean brightness error bi-histogram equalization in contrast enhancement, *IEEE Trans. Consum. Electron.* 49 (4) (2003) 1310–1319.
- [5] Chen Hee Ooi, Nor Ashidi Mat Isa, Quadrants dynamic histogram equalization for contrast enhancement, *IEEE Trans. Consum. Electron.* 56 (4) (2010).
- [6] Jing Rui Tang, Nor Ashidi Mat Isa, Bi-histogram equalization using modified histogram bins, *Appl. Soft Comput.* 55 (2017) 31–43.
- [7] Sheeba Jenifer, S. Parasuraman, Amudha Kadirvelu, Contrast enhancement and brightness preserving of digital mammograms using fuzzy clipped contrast-limited adaptive histogram equalization algorithm, *Appl. Soft Comput.* 42 (2016) 167–177.
- [8] Justin Joseph, R. Periyasamy, A fully customized enhancement scheme for controlling brightness error and contrast in magnetic resonance images, *Biomed. Signal Process. Control* 39 (2018) 271–283.
- [9] John B. Zimmerman, Stephen M. Pizer, Edward V. Staab, J. Randolph Perry, William McCartney, Bradley C. Brenton, An evaluation of the effectiveness of adaptive histogram equalization for contrast enhancement, *IEEE Trans. Med. Imaging* 7 (4) (1988) 304–312.
- [10] S. Anand, R. Shantha Selva Kumari, S. Jeeva, T. Thivya, Directionlet transform based sharpening and enhancement of mammographic X-ray images, *Biomed. Signal Process. Control* 8 (4) (2013) 391–399.
- [11] Sima Sahu, Amit Kumar Singh, S.P. Ghrera, Mohamed Elhoseny, An approach for de-noising and contrast enhancement of retinal fundus image using CLAHE, *Opt. Laser Technol.* 110 (2019) 87–98.
- [12] Jong Kook Kim, Jeong Mi Park, Koun Sik Song, Hyun Wook Park, Adaptive mammographic image enhancement using first derivative and local statistics, *IEEE Trans. Med. Imaging* 16 (5) (1997) 495–502.
- [13] Ming Zeng, Youfu Li, Qinghao Meng, Ting Yang, Jian Liu, Improving histogram-based image contrast enhancement using gray-level information histogram with application to X-ray images, *Opt. – Int. J. Light Electron. Opt.* 123 (6) (2012) 511–520.
- [14] Chenyi Zhao, Zeqi Wang, Huanyu Li, Xiaoyang Wu, Shuang Qiao, Jianing Sun, A new approach for medical image enhancement based on luminance-level modulation and gradient modulation, *Biomed. Signal Process. Control* 48 (2019) 189–196.
- [15] Akash Gandhamal, Sanjay Talbar, Suhas Gajre, Ahmad Fadzil M. Hani, Dileep Kumar, Local gray level S-curve transformation – a generalized contrast enhancement technique for medical images, *Comput. Biol. Med.* 83 (2017) 120–133.
- [16] Damian Tohli, Jim S. Jimmy Li, Image enhancement by S-shaped curves using successive approximation for preserving brightness, *IEEE Signal Process. Lett.* 24 (8) (2017) 1247–1251.
- [17] Hasan Demirel, Gholamreza Anbarjafari, Mohammad N. Sabet Jahromi, Image equalization based on singular value decomposition, 23rd International Symposium on Computer and Information Sciences, 2008. ISCIS'08 (2008) 1–5.
- [18] Y. Yang, Z. Su, L. Sun, Medical image enhancement algorithm based on wavelet transform, *Electron. Lett.* 46 (2) (2010) 120–121.
- [19] Hasan Demirel, Cagri Ozcinar, Gholamreza Anbarjafari, Satellite image contrast enhancement using discrete wavelet transform and singular value decomposition, *IEEE Geosci. Remote. Sens. Lett.* 7 (2) (2010) 333–337.
- [20] Fathi Kallel, Ahmed Ben Hamida, A new adaptive gamma correction based algorithm using DWT-SVD for non-contrast CT image enhancement, *IEEE Trans. Nanobioscience* 16 (8) (2017) 666–675.
- [21] Shanto Rahman, Md Mostafijur Rahman, Mohammad Abdullah-Al-Wadud, Golam Dastegir Al-Quaderi, Mohammad Shoyaib, An adaptive gamma correction for image enhancement, *EURASIP J. Image Video Process.* 2016 (1) (2016) 35.
- [22] A.K. Bhandari, Anil Kumar, G.K. Singh, Vivek Soni, Dark satellite image enhancement using knee transfer function and gamma correction based on DWT-SVD, *Multidimens. Syst. Signal Process.* 27 (2) (2016) 453–476.
- [23] A.K. Bhandari, A. Kumar, G.K. Singh, Improved knee transfer function and gamma correction based method for contrast and brightness enhancement of satellite image, *AEU-Int. J. Electron. Commun.* 69 (2) (2015) 579–589.
- [24] Zhenghua Huang, Tianxu Zhang, Qian Li, Hao Fang, Adaptive gamma correction based on cumulative histogram for enhancing near-infrared images, *Infrared Phys. Technol.* 79 (2016) 205–215.
- [25] A.K. Bhandari, V. Soni, A. Kumar, G.K. Singh, Cuckoo search algorithm based satellite image contrast and brightness enhancement using DWT-SVD, *ISA Trans.* 53 (4) (2014) 1286–1296.
- [26] Dervis Karaboga, Bahriye Akay, A comparative study of artificial bee colony algorithm, *Appl. Math. Comput.* 214 (1) (2009) 108–132.
- [27] Seyedali Mirjalili, Seyed Mohammad Mirjalili, Andrew Lewis, Grey wolf optimizer, *Adv. Eng. Softw.* 69 (2014) 46–61.
- [28] Seyedali Mirjalili, Amir H. Gandomi, Seyedeh Zahra Mirjalili, Shahrooz Saremi, Hossam Faris, Seyed Mohammad Mirjalili, Salp Swarm Algorithm: a bio-inspired optimizer for engineering design problems, *Adv. Eng. Softw.* 114 (2017) 163–191.
- [29] Amir Hossein Gandomi, Amir Hossein Alavi, Krill herd: a new bio-inspired optimization algorithm, *Commun. Nonlinear Sci. Numer. Simul.* 17 (12) (2012) 4831–4845.
- [30] Chandrasekaran Raja, Narayanan Gangatharan, A hybrid swarm algorithm for optimizing glaucoma diagnosis, *Comput. Biol. Med.* 63 (2015) 196–207.
- [31] Ebenezer Daniel, J. Anitha, Optimum wavelet based masking for the contrast enhancement of medical images using enhanced cuckoo search algorithm, *Comput. Biol. Med.* 71 (2016) 149–155.
- [32] Ebenezer Daniel, Optimum wavelet based homomorphic medical image fusion using hybrid genetic–Grey Wolf optimization algorithm, *IEEE Sens. J.* (2018).
- [33] Munendra Singh, Ashish Verma, Neeraj Sharma, Bat optimization based neuron model of stochastic resonance for the enhancement of MR images, *Biocybern. Biomed. Eng.* 37 (1) (2017) 124–134.
- [34] Salim Lahmiri, Mounir Boukadoum, A weighted bio-signal denoising approach using empirical mode decomposition, *Biomed. Eng. Lett.* 5 (2) (2015) 131–139.
- [35] Salim Lahmiri, Mounir Boukadoum, Physiological signal denoising with variational mode decomposition and weighted reconstruction after DWT thresholding, in: 2015 IEEE International Symposium on Circuits and Systems (ISCAS), IEEE, 2015, pp. 806–809.
- [36] Salim Lahmiri, An iterative denoising system based on Wiener filtering with application to biomedical images, *Opt. Laser Technol.* 90 (2017) 128–132.
- [37] Salim Lahmiri, Mounir Boukadoum, Combined partial differential equation filtering and particle swarm optimization for noisy biomedical image segmentation, in: 2016 IEEE 7th Latin American Symposium on Circuits & Systems (LASCAS), IEEE, 2016, pp. 363–366.
- [38] Bo Li, Wei Xie, Adaptive fractional differential approach and its application to medical image enhancement, *Comput. Electr. Eng.* 45 (2015) 324–335.
- [39] Shao-Hu Peng, Deok-Hwan Kim, Seok-Lyong Lee, Myung-Kwan Lim, Texture feature extraction based on a uniformity estimation method for local brightness and structure in chest CT images, *Comput. Biol. Med.* 40 (11–12) (2010) 931–942.
- [40] Salim Lahmiri, Image denoising in bidimensional empirical mode decomposition domain: the role of Student's probability distribution function, *Healthc. Technol. Lett.* 3 (1) (2015) 67–71.
- [41] Salim Lahmiri, Mounir Boukadoum, Biomedical image denoising using variational mode decomposition, in: 2014 IEEE Biomedical Circuits and Systems Conference (BioCAS) Proceedings, IEEE, 2014, pp. 340–343.
- [42] Salim Lahmiri, Denoising techniques in adaptive multi-resolution domains with applications to biomedical images, *Healthc. Technol. Lett.* 4 (1) (2017) 25–29.
- [43] Shilpa Suresh, Shyam Lal, Chintala Sudhakar Reddy, Mustafa Serbet Kiran, A novel adaptive cuckoo search algorithm for contrast enhancement of satellite images, *IEEE J. Sel. Top. Appl. Earth Obs. Remote. Sens.* 10 (8) (2017) 3665–3676.
- [44] Krishna Gopal Dhal, Sanjoy Das, A dynamically adapted and weighted Bat algorithm in image enhancement domain, *Evol. Syst.* (2018) 1–19.
- [45] Rencan Nie, Min He, Jinde Cao, Dongming Zhou, Zifei Liang, Pulse coupled neural network based MRI image enhancement using classical visual receptive field for smarter mobile healthcare, *J. Ambient Intell. Humaniz. Comput.* (2018) 1–12.